XXXVI Ibero-Latin American Congress on Computational Methods in Engineering
CILAMCE
Rio de Janeiro, 22-25 Nov 2015

EULER-EULER CFD STUDY OF HEAT TRANSFER IN FLUIDIZED BEDS WITH AN IMMERSED SURFACE USING THE KINETIC THEORY OF GRANULAR FLOWS

Me. Priscilla Corrêa Bisognin

Me. José Mozart Fusco

Dr[a]. Cíntia Soares

priscilla.cbisognin@gmail.com

cintia.soares@ufsc.br

Affiliation

Federal University of Santa Catarina, University Campus Reitor João David Ferreira Lima, 88040-970, SC, Florianópolis, Brazil

Second Author

mozart@esss.com.br

Affiliation

ESSS – Engineering Simulation and Scientific Software, 20210-031, RJ, Rio de Janeiro, Brazil

Abstract. *CFD simulations of a fluidized bed with an immersed heated surface were carried out using the Eulerian approach along with the kinetic theory of granular flows in order to investigate the best drag model, specularity coefficient and turbulence model to describe the surface-to-bed heat transfer and the hydrodynamics of the bed. Four different drag models were tested (Gidaspow, Syamlal & O'Brien, Wen & Yu and Beetstra). Gidaspow model was able to capture the solids distribution along the bed and also resulted in the best heat transfer model when compared with an experimental result. Six values of the specularity coefficient were evaluated as the boundary condition for the solid phase and the best results were obtained with the value of 0.1. Finally, the RNG* $\kappa - \varepsilon$ *dispersed model was included and improved the results for the heat transfer coefficient.*

Keywords: *Fluidization, Surface-to-bed heat transfer, CFD simulation, Drag model, Specularity coefficient.*

INTRODUCTION

Several processes are used in chemical industries, including mixture, drying, chemical reactions, heating and coating. All these processes can be made in fluidized beds, proving that this equipment is one of the most versatile in chemical engineering. Despite its vast use in the industry, engineers and researchers still encounter difficulties in understanding and modeling the complex phenomena occurring inside this equipment. This fact is due to the fluid-like behavior of the solids inside the bed, which turns the hydrodynamics into a complicated phenomenon.

The computational fluid dynamics (CFD) comprises numerical techniques to solve the constitutive equations of fluid flows. Since its creation, in the last century, this tool has been helping scientists to obtain information about the phenomena that occur inside equipments, which was not possible before. Among these phenomena is the heat transfer between a fluidized bed and an immersed heated surface.

The rapid movement of particles inside fluidized beds generates high rates of heat and mass transfer, one of the main characteristic of this type of bed. When the processes encompass chemical reaction a high rate of heat transfer is extremely desirable. This is the main reason why fluidized beds are used for so many types of chemical reactions, such as fluid catalytic cracking, synthesis reactions, combustion and gasification. To support endothermic reaction, heated surfaces are usually inserted in fluidized beds. A reliable computational model of this process would allow to gain information more rapidly and to realize a more guaranteed scale up. For these reasons the modeling of this process using CFD techniques has gained emphasis in the last years.

Two different approaches are commonly used when working with CFD techniques. The first one, named Lagrangean approach is based in the molecular dynamics, tracking the individual motion of each particle. This method requires large computational effort, being impracticable for industrial cases. The second one is called Eulerian approach and is much more common to describe fluidized bed problems. This approach considers both phases as interpenetrating continuum and requires less computational effort.

One of the main aspects of the fluidized bed is the fluid-like behavior of the particles. To describe this behavior the kinetic theory of granular flows (KTGF) is usually employed. This theory makes an analogy with the kinetic theory of gases, in order to describe the rheology of the particulate phase. Another important aspect to analyze in CFD simulations of gas-solid flows, such as the fluidized bed, is the boundary condition for the particulate phase. The specularity coefficient is an important parameter that describes the tangential momentum transfer due to collision of particles on the wall. The value of this coefficient varies between 0 and 1. The value of 0 corresponds to a free-slip condition and a value of 1 corresponds to a no-slip condition. Intermediate values represent a partial slip condition. Usually partial or no-slip conditions are used in fluidized bed simulations using the Eulerian approach, however the specularity coefficient has to be analyzed for each individual case.

Several authors have used the Eulerian approach along with the KTGF to investigate the behavior of fluidized beds, but there is still no global agreement concerning the best setup to perform such studies, especially when a heat transfer surface is inserted. Lungu et al. (2014) studied the influence of several parameters (drag model, heat transfer model, particle size and gas velocity) in the heat transfer coefficient inside a bubbling bed. Guan et al. (2014) used the Eulerian-granular model to investigate the effect of drag model in the hydrodynamics of a circulating fluidized bed for chemical looping combustion. Also using the Eulerian approach, Gan et al. (2012) investigated the particle segregation pattern in a gas-solid fluidized bed using different drag models. Xue e Fox (2014) used CFD techniques to model biomass gasification. Armstrong, Gu & Luo (2010) studied the influence of multiple heated tubes immersed in a fluidized bed in the heat transfer coefficient through the Eulerian-granular model.

Due to the importance of the heat transfer process between a heated surface and a fluidized bed to the chemical industry, this work has the aim of studying the best setup to investigate this phenomenon, using CFD techniques. For this, several drag models, specularity coefficients and a turbulence model were tested.

1 NUMERICAL SIMULATION

The influence of several parameters in the simulation of gas-solid fluidized beds was studied using the Eulerian approach and the kinetic theory of granular flows. The mathematical modeling and computational setup used in this study are covered in this section.

1.1 Governing equations

The Euler-Euler model is also referred to as two-fluid model, because it models both phases as fluids, considering the phases as interpenetrating continua. This model solves the classical conservation equations for both phases. The conservation equations for each phase are coupled with the appropriate constitutive equations. The continuity equations for gas and solid phases are given bellow:

$$\frac{\partial}{\partial t}\left(\alpha_g \rho_g\right) + \nabla \cdot \left(\alpha_g \rho_g \vec{v}_g\right) = 0 \tag{1}$$

$$\frac{\partial}{\partial t}\left(\alpha_s \rho_s\right) + \nabla \cdot \left(\alpha_s \rho_s \vec{v}_s\right) = 0, \tag{2}$$

where α is the volume fraction, ρ is the density, $\vec{v}_s$ is the velocity vector , the subscripts g and s refer to the gas and solid phase, respectively and $\nabla \cdot$ represents the divergence operator. The momentum equations are given as follow:

$$\frac{\partial}{\partial t}\left(\alpha_g \rho_g \vec{v}_g\right) + \nabla \cdot \left(\alpha_g \rho_g \vec{v}_g \vec{v}_g\right) = -\alpha_g \nabla p + \nabla \cdot \bar{\bar{\tau}}_g + \alpha_g \rho_g g + K_{gs}\left(\vec{v}_s - \vec{v}_g\right) \tag{3}$$

$$\frac{\partial}{\partial t}\left(\alpha_s \rho_s \vec{v}_s\right) + \nabla \cdot \left(\alpha_s \rho_s \vec{v}_s \vec{v}_s\right) = -\alpha_s \nabla p - \nabla p_s + \nabla \cdot \bar{\bar{\tau}}_s + \alpha_s \rho_s g + K_{gs}\left(\vec{v}_g - \vec{v}_s\right), \tag{4}$$

where p is the hydrodynamic pressure, $\bar{\bar{\tau}}$ is the viscous stress tensor, g is the acceleration due to gravity, K_{gs} is the momentum transfer between gas and solid phases and p_s is the solid phase pressure. The stress tensor for gas and solid phases is:

$$\bar{\bar{\tau}}_g = \alpha_g \mu_g \left(\nabla \vec{v}_g + \nabla \vec{v}_g^T\right) - \frac{2}{3}\alpha_g \mu_g \left(\nabla \cdot \vec{v}_g\right)\bar{\bar{I}} \tag{5}$$

$$\bar{\bar{\tau}}_s = \alpha_s \mu_s \left(\nabla \vec{v}_s + \nabla \vec{v}_s^T\right) - \alpha_s \left(\lambda_s - \frac{2}{3}\mu_s\right)\left(\nabla \cdot \vec{v}_s\right)\bar{\bar{I}}\ , \tag{6}$$

where μ_s is the solid shear viscosity and λ_s is the solid bulk viscosity. In this work the momentum exchange, K_{gs}, is based on Gidaspow's model (1994) and the viscosity and pressure of the solid phase is obtained with the kinetic theory of granular flow (KTGF) (Gidaspow, 1994). The solid bulk viscosity and solid pressure are given by Lun et al. (1984) and the solid shear viscosity is given by Gidaspow (1994).

The shear force at the wall for the granular phase is given by:

$$\overline{\tau_s} = \frac{\pi}{6}\sqrt{3}\varphi \frac{\alpha_s}{\alpha_{s,\max}} \rho_s g_0 \overline{U_{S,||}} \sqrt{\Theta_s}\ , \tag{7}$$

where $\overline{U_{S,||}}$ is the particle slip velocity, parallel to the wall, φ is the specularity coefficient, Θ_s is the granular temperature, g_0 is the radial distribution function and $\alpha_{s,max}$ is the volume fraction for the particle at maximum packing, considered in this work as 0.64 (Kamien & Liu, 2007).

The energy accumulation in both phases due to convection, diffusion and interphase heat transfer constitutes the thermal energy balance, given by:

$$\frac{\partial}{\partial t}\left(\alpha_g \rho_g H_g\right) + \frac{\partial}{\partial x_i}\left(\alpha_g \rho_g U_{i,g} H_g\right) = \frac{\partial}{\partial x_i}\left(\alpha_g k_g \frac{\partial T_g}{\partial x_i}\right) + \gamma_v \left(T_s - T_g\right) \tag{8}$$

$$\frac{\partial}{\partial t}\left(\alpha_s \rho_s H_s\right) + \frac{\partial}{\partial x_i}\left(\alpha_s \rho_s U_{i,s} H_s\right) = \frac{\partial}{\partial x_i}\left(\alpha_s k_s \frac{\partial T_s}{\partial x_i}\right) + \gamma_v \left(T_g - T_s\right), \tag{9}$$

where k is the thermal conductivity, H is the enthalpy, γ_v is the interphase volumetric heat transfer coefficient and T is the temperature.

The heat transfer is accounted through the Nusselt number. In this work the heat transfer model of Gunn (1978) was used:

$$\begin{aligned} Nu_s = {} & \left(7 - 10\alpha_g + 5\alpha_g^2\right)\left(1 + 0.7\left(\mathrm{Re}_p\right)^{0.2}\left(\mathrm{Pr}\right)^{1/3}\right) + \\ & \left(1.33 - 2.40\alpha_g + 1.20\alpha_g^2\right)\left(\mathrm{Re}_p\right)^{0.2}\left(\mathrm{Pr}\right)^{1/3} \end{aligned}\ , \tag{10}$$

where Pr is the Prandtl number, Re_p the particle Reynolds number and C_p the specific heat.

1.2 Numeric setup

All simulations were carried out using the Eulerian two-fluid model along with the kinetic theory of granular flows. The geometry in this study was based on the fluidized bed used in the experimental work of Di Natale, Lancia & Nigro (2007). A two-dimensional representation of a bed with 0.1 m width and 1.8 m height was developed. During the simulations it was considered the axisymmetry, in order to capture the heat dissipation along the perimeter of the bed. Initially a height of 0.6 m of the bed was filled with 500 μm diameter glass beads. The solids density is 2540 $kg{\cdot}m^{-3}$, the specific heat is 765 $j{\cdot}kg^{-1}{\cdot}k^{-1}$ and the conductivity is 0.9 $w{\cdot}m^{-1}{\cdot}k^{-1}$. The inlet gas velocity was maintained constant at 0.45 m/s. Inside the bed, at 0.3 m above the gas distributor, it was inserted a heat transfer surface (diameter 20 mm and height 30 mm). Figure 1 represents the geometry used in the studies, with the gravity acting in the horizontal coordinate.

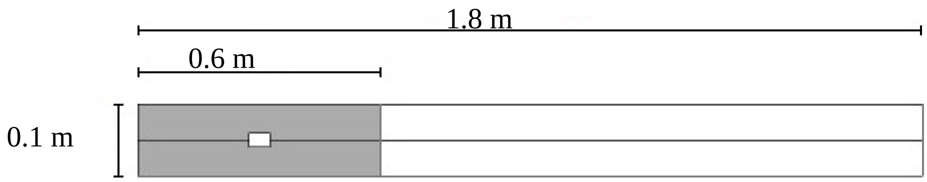

Figure 1. Horizontal representation of the bed geometry

1.3 Initial and boundary conditions

To study the heat transfer phenomena, a constant heat flux was set in the bed of the heat transfer surface, according to the experimental work of Di Natale, Lancia & Nigro (2007). At the inlet of the bed, gas was maintained at a constant velocity of 0.45 m/s. At the outlet of the bed the atmospheric pressure was considered. For the walls of the cylinder and the surface a no-slip condition was set to the gas phase and a partial slip condition was applied for the solid phase by testing different specularity coefficients (0; 0.05; 0.1; 0.25; 0.5 and 1).

1.4 Solution procedure

The simulations were performed in the CFD package ANSYS® CFD (FLUENT®) v. 15.0, that uses the finite volume method for solving a set of governing equations. The implicit pressure-based solver and the phase coupled SIMPLE scheme for pressure-velocity coupling were used. The simulation were carried for a time of 20 s, and all the averaged results were calculated using the last 15 s of simulation, since the results of the beginning of the simulation are not stable, due to startup effects. The transient nature of the fluidization must exhibit a cyclic pattern of parameter fluctuations, due to solids motion, which begins to occur after 5 s. A small time step of $2{\cdot}10^{-4}$ s was chosen to prevent instabilities and ensure a quick convergence (Armstrong, Gu & Luo , 2010). The convergence criterion was set in $1{\cdot}10^{-3}$ and a second order scheme of discretization was applied for both time and space. Grid independence results were achieved with a structured grid with 0.0045 m element size, approximately 10 times the particle size, which is in good agreement with other authors (Li; Benyahia, 2013; Kong; Zhang; Zhu, 2014).

2 RESULTS AND DISCUSSION

In order to determine the best CFD setup to describe the heat transfer phenomena between a fluidized bed and an immersed surface, the heat transfer coefficient was analyzed for different specularity coefficients, drag models and a turbulence model.

2.1 Drag model

The drag force is one of the main forces acting in a fluidized bed and is the one that is responsible for the fluidization phenomena. It appears due to the velocity difference between the phases and is a function of the Reynolds number and the solids volumetric fraction. The importance of this force to the fluidization phenomena reflects directly in the importance of the choice of drag model. Most drag models have an empiric base, but authors have been recently using results from lattice-Boltzmann simulations to generate drag models (Hill, Koch & Ladd, 2001; Beetstra, 2005).

In this work four different drag models were tested: Wen & Yu (1966), Gidaspow (1986), Syamlal & O'Brien (1989) and Beetstra (2005). Figure 2 shows the instantaneous solids distribution after 20 s of simulation. In this figure the blue areas represent the gas phase and the red areas represent the maximum packing.

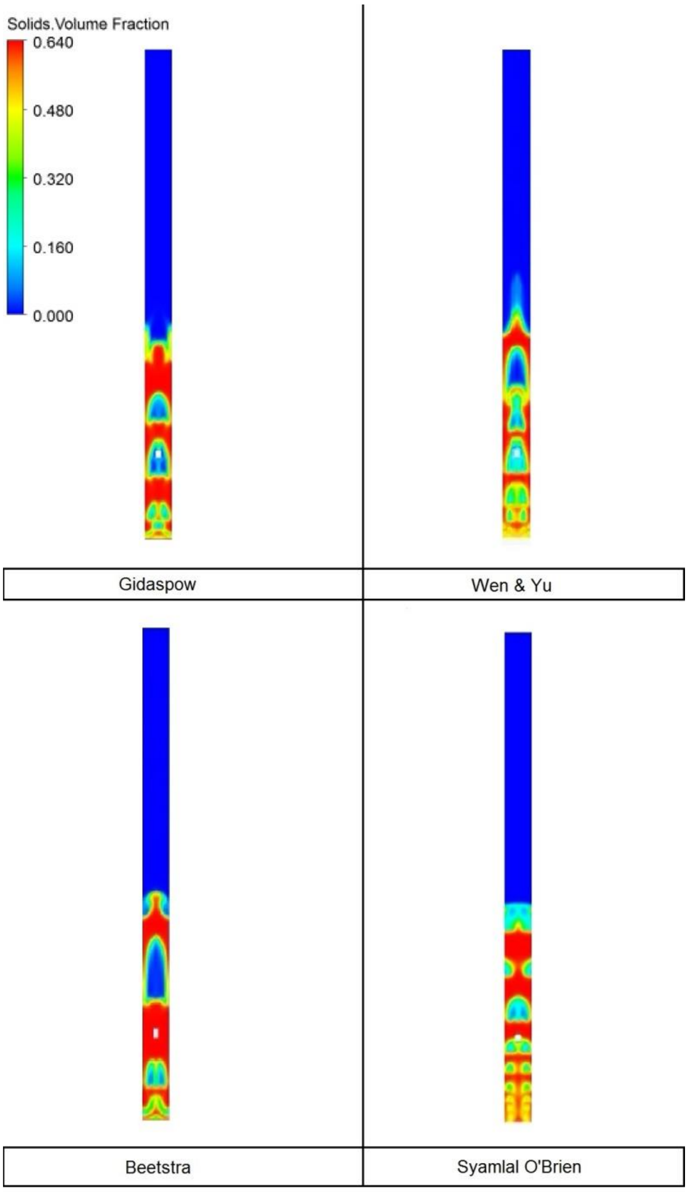

Figure 2: Bubble patterns for different drag models, after 20 s of simulation.

Analyzing Figure 2 is possible to note that the only drag model that results in a disparate behavior concerning the solids pattern is the Syamlal & O'Brien drag model. The train of bubbles observed in the simulation using this drag model does not correspond to the physical behavior of a fluidized bed. All other drag models resulted in a classical bubble shape. The classic article by Werther and Molerus (1973) presents the pattern of bubbles for Geldart B solids, where small bubbles are formed close to the distributor and tend to move to the center of the bed and coalesce. When the diameter of the bed is small compared to its height, the bubble growth is limited by the column wall, characterizing the slugging regime. According to De Lasa (1986) the bubbles in the slugging regime assume an axisymetric bullet shape, like the one presented in Figure 2 for all drag models, except for Syamlal & O'Brien.

The main mechanism of heat transfer inside bubbling beds is the convective heat transfer. For that reason is also necessary to investigate the effect of the drag model in the heat transfer coefficient. Table 1 displays the time-averaged heat transfer coefficient for the drag models tested:

Table 1. Heat transfer coefficient for different drag models.

Model	Time-averaged heat transfer coefficient ($W/m^2 \cdot K$)
Gidaspow (1986)	171.10
Syamlal & O'Brien (1989)	158.58
Wen & Yu (1966)	142.77
Beetstra (2005)	142.65

In order to determine the drag model that resulted in the best drag model coefficient for the simulation of this particular case, the results presented in Table 1 were compared with the experimental result of Di Natale et al. (2007) (230 $W/m^2 \cdot K$). For this study Gidaspow drag model was chosen because it resulted in a realistic description of the hydrodynamics of the bed and it also provided a better prediction of the heat transfer coefficient. The Gidaspow model was chosen to proceed the simulation in next sections. The underestimation of the heat transfer was probably due to an underprediction in the solids fraction around the heated cylinder.

2.2 Specularity coefficient

The specularity coefficient describes the boundary condition for the solid phase and is related to the tangential momentum transfer between particles and the wall. The value of this parameter varies between 0 and 1. The specularity coefficient is related to the shear stress at the wall, according to Eq. (7). When the specularity coefficient is zero the boundary is a smooth frictionless wall and no shear stress is exerted.

Commonly intermediate values are used for fluidized beds simulations, characterizing a partial slip condition. For bubbling beds, lower values are recommended by the technical literature (Li & Benyahia, 2013), although there is no agreement concerning a global value to be used in bubbling beds simulations. To understand the influence of this parameter and define the best value to be used in this specific case, six values of specularity coefficient were tested (0, 0.05,0 0.1, 0.25, 0.5 e 1). Figure 3 shows the time-averaged solids fraction along the height of the bed and Fig. 4 shows the instantaneous solids distribution in the bed in different moments of the simulation.

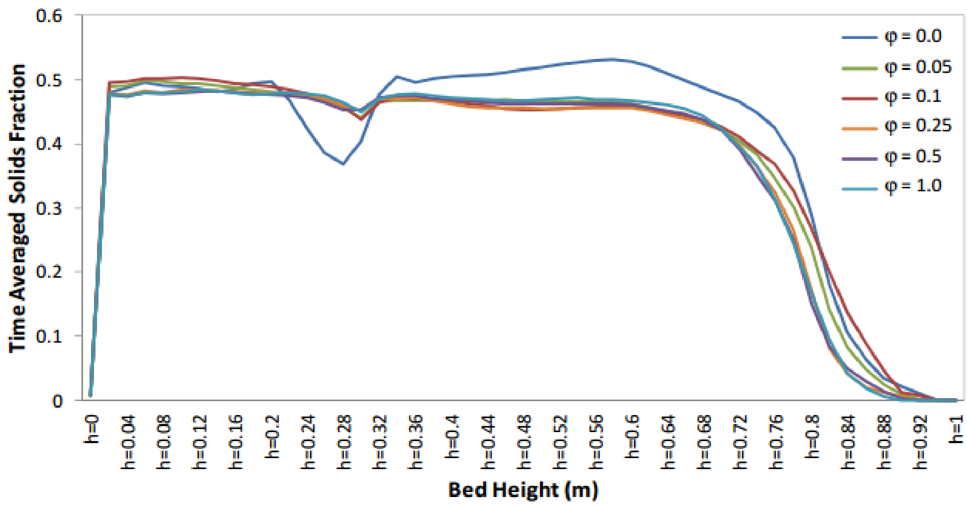

Figure 3. Time-averaged solids fraction for along the bed height for different specularity coefficients.

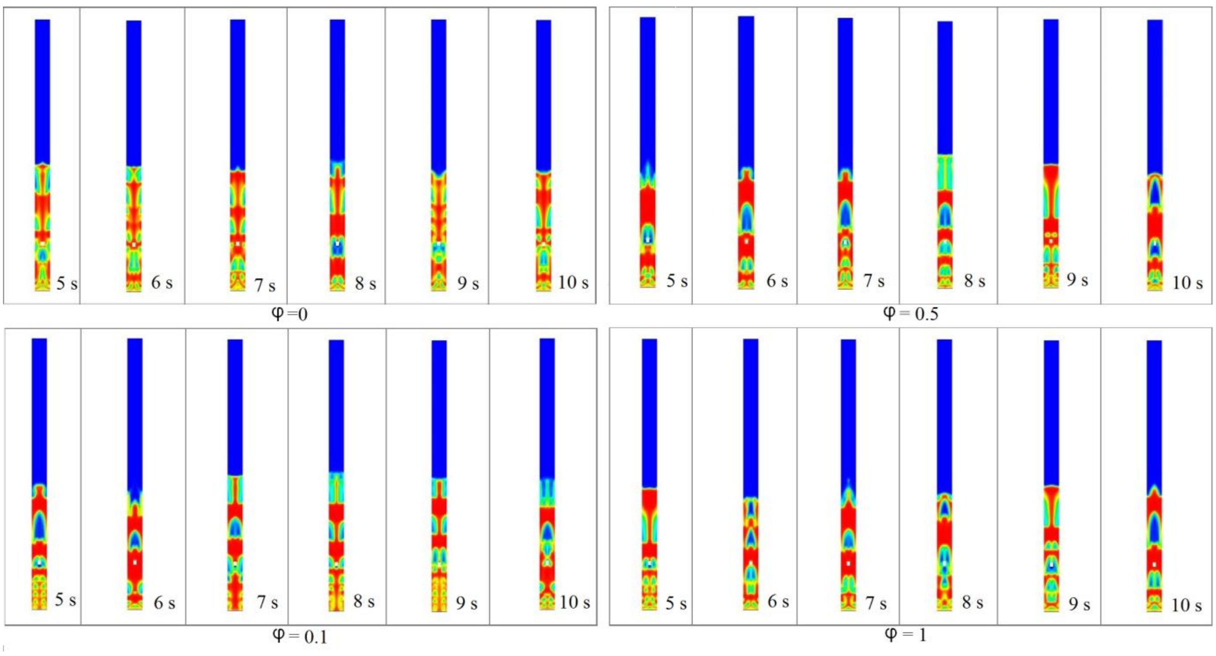

Figure 4. Time-averaged solids fraction for along the bed height for different specularity coefficients.

Fig. 4 presents the solids fraction distribution along the bed, where the color red represents the maximum packing of solids and the color blue the absence of solids. The results contained in Fig. 3 and Fig. 4 present clearly how the hydrodynamics of the bed is altered by the specularity coefficient. When this parameter is 0 (free-slip condition) the behavior of the solids is different from the pattern observed for other values. In Fig. 3 there is a sudden decrease in the solids fraction, and after that, the solids fraction increases. This does not correspond to the expected physical behavior of a fluidized bed, in which the solids fraction tends to diminish along the height. Fig. 4 also shows how the free-slip condition diverges from the partial and no-slip conditions. For this case the instantaneous solids distribution shows a train of bubble in the wall of the bed, which also does not correspond to the physical behavior of a bubbling bed.

The next step in the specularity coefficient evaluation was to compare the heat transfer coefficient obtained with different specularity coefficient values with the experimental result encountered by Di Natale, Lancia & Nigro (2007), 230 W/m²·K. This comparison is showed in Table 2, as follows:

Table 2. Heat transfer coefficient for different specularity coefficients.

Specularity coefficient	Time-averaged heat transfer coefficient (W/m²·K)	Deviation from the experimental data from Di Natale , Lancia & Nigro (2007)
$\varphi = 0$	163.10	29.09%
$\varphi = 0.05$	175.27	23.80%
$\varphi = 0.1$	175.94	23.51%
$\varphi = 0.25$	140.39	38.96%
$\varphi = 0.5$	154.72	32.73%
$\varphi = 1$	136.39	40.70%

Although there is little variation in the bed hydrodynamics, as shown in Fig. 3 and Fig. 4, Table 2 proves that the specularity coefficient has a great influence on the heat transfer coefficient, with the value of 0.1 presenting the result closest to the experiment. Li et al. (2010) suggested that the specularity coefficient is influenced by the gas velocity and for that reason is impossible to establish on global value for all fluidized bed simulations. The best practice to determine this parameter is to compare simulation results with experimental data.

2.3 Turbulence model

The next step in the evaluation of the best setup for simulating the case of a fluidized bed with an immersed heated surface was the inclusion of a turbulence model. The model chosen was the RNG κ-ε with dispersed multiphase model. Figure 5 shows the solids distribution in different times of the simulated bed with the turbulence model. Table 3 displays the results for the time-averaged heat transfer coefficient with and without the presence of the turbulence model, and compares these results with the experimental data of Di Natale et al. (2007).

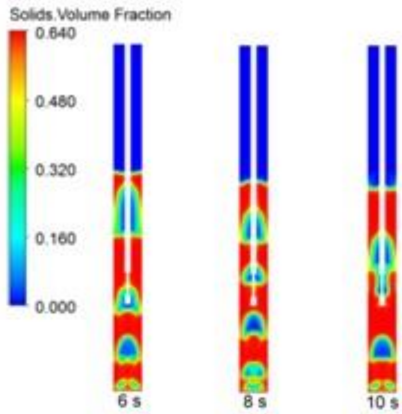

Figure 5: Transient solids distribution with the inclusion of the turbulence model.

Table 3. Heat transfer coefficient for with the inclusion of a turbulence model.

Turbulence model	Time-averaged heat transfer coefficient (W/m²·K)	Deviation from the experimental data from Di Natale et al. (2007)
Laminar	175.94	23.51%
RNG κ-ε dispersed	207.02	9.99%

The addition of the turbulence model did not affect the shape of the bubble, that still presents the same bullet shape as presented in Figure 2, but had a great impact on the heat transfer coefficient. For that reason it is advisable that a proper turbulence model should be used in heat transfer problems in fluidized bed, as the inclusion of this model turns the simulations more realists and generates more reliable results.

Using average values of gas velocity, the resulting Reynolds number is around 2300. Even though this process is turbulent, the initial steps of the research (study of drag model and specularity coefficient) are valid because they intend to evaluate primarily the solids distribution along the bed and its relation to the heat transfer. The bubble pattern was not altered due to inclusion of the turbulence model, but its addition made possible for the overall model to capture the mixing due to the eddy formation, which consequently increases the heat transfer.

3 CONCLUSION

In recent years engineers and researchers have been using numerical simulation to understand and scale up innumerous processes. Fluidized beds are complex equipments that present phenomena difficult to model. After these studies it was defined that a setup comprising the Gidaspow drag model, specularity coefficient of 0.1 and RNG κ-ε dispersed turbulence model was ideal to describe the case proposed. The specularity coefficient is related to the boundary condition at the walls of the bed and the heated cylinder, therefore its definition will affect the description of the solids movement which leads to a change in the heat transfer coefficient. The inclusion of the turbulence model was essential to improve the numerical description of the problem, since the formation of vortices improves the mixing and consequently the heat transfer in the bed. The importance of these findings rely on the fact that this setup can be used to investigate different parameters of the bed in the heat transfer phenomena, such as gas velocity, particle size and geometry of the immersed surface.

ACKNOWLEDGEMENTS

The authors acknowledge CAPES for the financial support.

REFERENCES

Armstrong, L.M., Gu, S., Luo, K.H., 2010. The influence of multiple tubes on the tube-to-bed heat transfer in a fluidized bed. *International Journal of Multiphase Flow*, vol. 36, pp. 916–929.

Beetstra, R., 2005. *Drag force in random arrays of mono- and bidisperse spheres*. PhD thesis, Universiteit Twente/Netherlands

De Lasa, H., 1986. *Chemical Reactor Design and Technology*. Springer Netherlands.

Di Natale, F., Lancia, A., Nigro, R., 2007. Surface-to-bed heat transfer in fluidised beds: Effect of surface shape. *Powder Technology*, vol. 174, n. 3, pp. 75–81.

Gan, J. et al., 2012. Impact of the drag law formulation on the predicted binary-particle segregation pattern in a gas-solid fluidized bed. *Powder Technology*, vol. 218, pp. 69–75.

Gidaspow, D., 1986. Hydrodynamics of fluidization and heat transfer: supercomputer modeling. *Applied Mechanics Reviews*, vol. 39, pp. 1–23.

Gidaspow, D., 1994. Multiphase flow and fluidization: Continuum and kinetic theory descriptions. Academic Press.

Guan, Y. et al., 2014. Three-dimensional CFD simulation of hydrodynamics in an interconnected fluidized bed for chemical looping combustion. *Powder Technology*, vol. 268, pp. 316–328.

Gunn, D. J., 1978. Transfer of heat or mass to particles in fixed and fluidized beds. *International Journal of Heat and Mass Transfer*, vol.21, pp. 467-476.

Hill, R., Koch, D., Ladd, A., 2001. The first effects of fluid inertia on flows in ordered and random arrays of spheres. *Journal of Fluid Mechanics*, vol. 448, pp. 213–241.

Kamien, R. D., Liu, A. J., 2007. Why is random close packing reproducible? *Physical Review Letters*, vol. 99, pp. 155501.

Kong, L.; Zhang, C.; Zhu, J., 2014. Evaluation of the effect of wall boundary conditions on numerical simulations of circulating fluidized beds. *Particuology*, vol. 13, pp. 114–123.

Li, T.; Benyahia, S., 2013 Evaluation of wall boundary condition parameters for gas-solids fluidized bed simulations. *AIChE Journal*, vol. 59, pp. 3624–3632.

Li, T., Grace, J., Bi, X., 2010. Study of wall boundary condition in numerical simulations of bubbling fluidized beds. *Powder Technology*, vol. 203, pp. 447–457.

Lun, C. K. K. et al., 1984. Kinetic theories for granular flow: inelastic particles in couette flow and slightly inelastic particles in a general flow field. *Journal of Fluid Mechanics*, vol. 140, pp. 223–256.

Lungu et al., 2014. Computational fluid dynamics simulations of interphase heat transfer in a bubbling fluidized bed. *Korean Journal of Chemical Engineering,* vol. 31, n. 7, pp. 1148–1161.

Syamlal, M., O'Brien, T., 1989. Computer simulation of bubbles in a fluidized bed. *AIChE Symposium Series.*, vol. 85, p. 22–31.

Wen, C.Y., Yu, Y. H., 1966. Mechanics of fluidization. *Chemical Engineering Progress Symposium Series*, vol. 62, pp. 100–111.

Werther J., Molerus O., 1973. The local structure of gas fluidized beds-II. The spatial distribution of bubbles. *International Journal of Multiphase Flow*, vol.1, pp. 123–138.

Xue, Q., Fox, R., 2014. Multi-fluid CFD modeling of biomass gasification in polydisperse fluidized-bed gasifiers. *Powder Technology*, vol. 254, pp. 187–198.